Food Packaging and Shelf Life 53 (2026) 101711

Contents lists available at ScienceDirect

Food Packaging and Shelf Life

journal homepage: www.elsevier.com/locate/fpsl

Influence of uniaxial orientation on oxygen barrier properties of polyethylene films

Dixit Guleria [a,b,c], Dimitri Adons [d], Jaap den Doelder [c,e,*], Roos Peeters [d], Peter Ragaert [a]

[a] Faculty of Bioscience Engineering, Department of Food Technology, Safety and Health, Ghent University, Coupure Links 653, Gent 9000, Belgium
[b] Centre for Polymer and Material Technologies (CPMT), Department of Materials, Textiles and Chemical Engineering, Ghent University, Technologiepark 130, Zwijnaarde 9052, Belgium
[c] Laboratory of Physical Chemistry (SPC), Department of Chemical Engineering and Chemistry, Eindhoven University of Technology,Groene Loper 3, Eindhoven 5612 AE, the Netherlands
[d] Hasselt University, Institute for Materials Research (imo-imomec), Materials and Packaging: Research & Services (MPR&S), Martelarenlaan 42, Hasselt B-3500, Belgium
[e] Dow Benelux B.V., Packaging and Specialty Plastics, P.O. Box 48, Terneuzen 4530 AA, the Netherlands

ARTICLE INFO

Keywords:
Design for recycling
Flexible packaging
Circular Packaging
Oxygen barrier
PE Blown films
MDO-PE films
Mono-material design

ABSTRACT

The transition from traditional materials like glass and metal to plastic films in food packaging has been driven by the latter's flexibility, versatility, and lightweight nature. However, challenges related to the recycling of multi-layered, multi-material flexible packaging have emerged, prompting interest in mono-material solutions for improved recycling and sustainability. Polyethylene (PE), a widely used polymer in flexible packaging, offers various structural and functional properties but faces issues with high oxygen permeability. This study investigates the potential of uniaxial orientation or machine direction orientation (MDO) to enhance the oxygen barrier property of PE films. Oxygen barrier properties were evaluated for blown and MDO films of varying resin densities, with the results correlating structural changes during stretching with improved barrier performance at a certain resin and process parameters. The findings demonstrated that uniaxial orientation or MDO operation has the potential to enhance the oxygen barrier of PE films, depending on resin type and processing conditions, primarily through enhanced crystallinity and microstructural orientation.

1. Introduction

Historically, the predominant materials utilized for food packaging have included glass, metals (such as aluminium foil, tin-free steel), and various types of coated papers (Guzman-Puyol et al., 2022; Risch, 2009). Metal packaging ensures a long shelf life by blocking microbes, light, and oxygen, while glass offers inert, nontoxic protection with excellent barrier properties; however, both are increasingly being replaced by plastics due to their flexibility, versatility, thermal stability, and lightweight nature.

Polymers are extensively utilized in contemporary food and beverage packaging industries (Chatterjee et al., 2014). Plastic packaging materials play a crucial role in the economy by preserving food, pharmaceuticals, and biomedical products (Jost, 2018; Qasim et al., 2021; Trinh et al., 2023).

The primary purpose of food packaging is to preserve food quality from production to consumer use (Chen et al., 2024; Lazić et al., 2010; Thomas et al., 2024). Effective barrier properties are essential for plastic films in food packaging to preserve nutritional and organoleptic qualities as well as safety of the product (Ayuso et al., 2017). Multi-layer configurations are widely used in food packaging for their superior performance, combining up to 11 layers to offer excellent mechanical resistance, thermal properties, sealing, and barriers against vapours, gases, and light (Carullo et al., 2023). However, multi-layer configurations pose significant recycling challenges due to difficulties in separating different plastic polymer types and the inability to recycle mixed polymers with diverse properties (Carullo et al., 2023; Dilkes-Hoffman et al., 2018; Faraca & Astrup, 2019).

A significant challenge in the mechanical recycling of flexible packaging plastic waste stems from its multi-layered structure, which

* Correspondence to: Laboratory of Physical Chemistry (SPC), Department of Chemical Engineering and Chemistry, Eindhoven University of Technology, Groene Loper 3, Eindhoven 5612 AE, the Netherlands.
E-mail addresses: Dixit.Guleria@UGent.be, d.guleria@tue.nl (D. Guleria), cfdendoelder@dow.com, C.F.J.d.Doelder@tue.nl (J. den Doelder), roos.peeters@uhasselt.be (R. Peeters), Peter.Ragaert@UGent.be (P. Ragaert).

https://doi.org/10.1016/j.fpsl.2026.101711
Received 23 October 2025; Received in revised form 7 January 2026; Accepted 24 January 2026
Available online 28 January 2026

often consists of diverse thin plastic film layers, such as polyethylene (PE), polypropylene (PP), polyamide (PA), polyethylene terephthalate (PET), and polyvinyl chloride (PVC), along with non-ferrous metals like aluminium and tin. Conventional plastic reprocessing techniques like mechanical recycling are ineffective for such multi-material, multi-layered configurations due to inherent chemical incompatibilities between the constituent layers (Barlow & Morgan, 2013; Ma, 2018). Thus, embedded heterogeneity of these flexible packaging systems poses significant challenges to current recycling systems, as conventional waste management infrastructure lacks the capability to effectively identify, sort, and recycle these complex materials, thereby undermining the principles of a circular economy (Dilkes-Hoffman et al., 2018; Faraca & Astrup, 2019; Kaiser et al., 2018; Soares et al., 2022; Walker et al., 2020).

To improve recycling rates, mono-material multi-layered flexible packaging systems are emerging as a new alternative. Still multiple variations are typically needed to achieve initial use-phase functionality, but as these materials are from one chemical composition, when mixed during recycling process steps, the resulting recycled product has good potential to perform well. Polyolefin-based mono-material flexible films have emerged as promising candidates for fulfilling the demands of a circular economy, owing to their ease of mechanical recyclability, as evidenced by numerous studies (Barlow & Morgan, 2013; Guerritore et al., 2022; Srebrenkoska et al., 2009). Polyethylene (PE) is one of the most used polymers in flexible packaging applications as it can provide various useful structural and functional properties (moisture barrier, good sealing because of low melting temperature, high impact resistance) because of its distinct available grades and types like low-density polyethylene (LDPE), linear low-density polyethylene (LLDPE), and high-density polyethylene (HDPE). There is promise in achieving both package functionality and recyclability when combining different grades of PE into a single package.

A major issue with polyethylene is its high oxygen permeability (Ayuso et al., 2017). The permeability of gases or moisture in polymers is influenced by the solubility and diffusion of the permeants, which is governed by factors such as crystallinity, polarity, and molecular weight (Trinh et al., 2023). Oxygen being apolar dissolve more into apolar polymers such as PE, PP and most polyolefins as compared to polar polymers such as PET and nylon (Varun Fotedar, 2022). The molecular structure of PET is composed of rigid aromatic benzene rings and polar ester group, creating polarity, which helps in tight intermolecular interactions whereas, the molecular structure of PE consists of long, apolar hydrocarbon chains with repeating (CH_2) units, which are relatively more flexible and are packed relatively less tightly. Polar groups cause polymer chains to be mutually attracted, which ultimately increase glass transition temperature and reduces free volume (Comyn, 2005). Therefore, due to relatively lesser free volume, PET has higher barrier for the diffusion of oxygen in comparison to PE. However, it has been demonstrated in previous studies that oxygen as well as moisture barrier of PE films can be enhanced by MDO operation (Breese & Beaucage, 2005; Chatterjee et al., 2014).

Traditionally, the outer layer of multilayer flexible packaging is composed of non-PE materials, such as PET or PA, which provide the overall package with sufficient stiffness and barrier properties. Orientation of PE film in the semi-solid state through techniques such as tenter frame, double bubble, and machine direction orientation significantly enhances its mechanical and barrier properties. This further facilitates the development of lightweight packaging structures (Paul et al., 2022), offering a viable alternative to move away from multi-material multi-layer structures.

During the MDO process, the precursor polymer film made from cast or blown film process is stretched further in the machine direction to a certain extent and at a certain rate and temperature which depends on the polymer's chemical nature. Consequently, numerous enhancements are observed in the physical and barrier properties of the films for food packaging applications, including stiffness, tensile strength, gloss, oxygen resistance, and moisture barrier (Chatterjee et al., 2014; Hatfield et al., 2002; W. Ma et al., 2024). During stretching a fibrillar structure with higher crystallinity is formed (Elias et al., 2000; Guleria, Edeleva, et al., 2024; Guleria et al., 2025; Guleria, Ge, et al., 2024; Tabatabaei, Carreau, et al., 2009; Tabatabaei, Parent, et al., 2009).

Multiple factors have been suggested to account for the enhanced barrier properties observed in oriented polymers. These include reduced free volume in amorphous regions, increased diffusion path tortuosity due to crystal alignment, and higher overall crystallinity, along with denser packing and microfibrillar crystal formation (Breese & Beaucage, 2005; Chatterjee et al., 2014; Paulos & Thomas, 1980; Sha & Harrison, 1992; Williams & Peterlin, 1971).

Chatterjee *et al.* (Chatterjee et al., 2014) investigated water vapor barrier of HDPE MDO films and reported that initially the oriented films demonstrated an increase in the water vapor transport rate with increasing draw ratio and beyond a critical draw ratio it gradually decreased. Breese *et al.* (Breese & Beaucage, 2005) investigated effect of MDO on the moisture and oxygen barrier properties of HMW (high molecular weight)-PE films and reported that a significant decrease in both moisture and oxygen transmission rates is observed with the machine direction orientation of homopolymer HMW-PE films. They further reported that intermediate and lower density films do not show such a significant decrease and actually present a maximum at moderate draw ratios where the transmission rate is greater after orientation than that of the undrawn sample.

Most of the studies mentioned to investigate the barrier properties are based on MDO process parameters like draw ratio but only few studies focus on the role of structural parameters of the resins like resin density and correlate it with changes in structural morphology during stretching. Therefore, oxygen barrier of the MDO-PE films was evaluated in this study and further correlated with resin density and film morphology while keeping the other MDO process parameters constant like draw ratio, orientation temperature and stretch rate.

2. Materials and methods

2.1. Materials

Five PE resins (D1, D2, D3, D4, D5) composed of ethylene copolymerized with an α-olefin, were provided by Dow for this study. The five PE resins were labelled in the order of increasing density, with D1 representing the resin with lowest density and resin D5 representing the resin with highest density. Resins D1, D3, and D4 are synthesized using similar catalyst chemistry, whereas D2 and D5 are based on hybrid catalyst chemistry. The measured density and melt flow index (MFI) of all five resins are presented in Table 5.1. The MFI was measured in accordance with ASTM D1238, using a Göttfert MI-4 plastometer with an average of 19 measuring points taken in a single measurement run for improved accuracy. The measurements were conducted under standard conditions for PE, (2.16 kg at 190 °C). Density measurements were conducted following the ASTM D792 protocol, using isopropyl alcohol (IPA) as the immersion liquid. The density values reported in Table 1 represent the average of three measurements.

Table 1
Characteristics of all the 5 base PE resins used in the study.

Resin	MFI (dg/min)	Density* (g/cm^3)
D1	1.020	0.9194 ± 0.0003
D2	1.872	0.9256 ± 0.0002
D3	1.472	0.9500 ± 0.0001
D4	4.102	0.9540 ± 0.0003
D5	1.126	0.9667 ± 0.0001

* Error is standard deviation in density column.

2.2. Base sheets and lab scale MDO stretching

Base sheets from all five base resins of approximately 550 microns thickness were prepared at 190 °C and 150 bar pressure using a Colin compression molding press, followed by quench cooling with circulating room temperature water through channels in the hot press plates. Rectangular specimens of 20 mm width and 100 mm in length were cut from the base sheet. The specimens were stretched under laboratory conditions using a Lloyd LR10K Plus tensile tester equipped with an environmental chamber to regulate the orientation temperature (Fig. 1). The 20 mm-wide strips were stretched to a fixed length draw ratio of 7, corresponding to an extension from 25 mm to 175 mm of grip separation. Stretching was conducted at a temperature of 110 °C with a constant rate of 200 mm/min. It is important to note that the optimal stretching or orientation temperature depends on the polymer's microstructural properties and may vary for different applications to achieve the desired results. Typically, orientation is performed at temperatures above the glass transition temperature and below the peak melting temperature, as higher orientation temperatures generally enable greater stretch ratios without film breakage (DeMeuse, 2011). Following the stretching process, the samples were annealed for 2 min at a fixed temperature of 120 °C. The annealing step freezes the orientation provided in the stretching step and stabilizes the film from further dimensional changes. After annealing, the films were cooled under ambient room temperature. In addition to five base resins, base sheets and lab-scale MDO films were produced from binary blends of low-density resin D2 and higher-density resin D5, with D2 proportions of 25 %, 50 %, and 75 % by weight, denoted as D2/D5 (25/75), D2/D5 (50/50), and D2/D5 (75/25). The densities of the blends were theoretically estimated using an approximate inverse-additive mixing rule. Resin D5 base sheet could not be stretched to the length draw ratio of 7 due to its extremely high density and crystallinity as compared to other resins and blends. Due to the high fraction of crystalline phase, its microstructure showed extreme fibrillation and necking during stretching at the used specific orientation temperature and thus ultimately broke off under tensile load.

2.3. Preparation of blown films

Blown films were produced using a LabTech blown film line (40 mm die diameter, 0.8 mm die gap) with a thickness of approximately 50 μm and a lay-flat width of ~145 mm (Figure S1 in supplementary information). The blow-up ratio (BUR) and draw-down ratio (DDR) were approximately 2.31 and 3.15, respectively, with a mass flow rate of approximately 30 g/min. The extruder temperature profile ranged from 160 °C to 190 °C, while the die outlet temperatures were 180 °C (lower) and 160 °C (upper). The nip roller speed was around 3 m/min, with slight adjustments to achieve the target BUR and DDR for each extrusion. After exiting the die, all blown films were cooled at similar rates at ambient room temperature under constant process parameters. The blown films were produced for all five base resins. The dry blending technique was employed to fabricate blown films of blends using resin D2 and D5 on the blown film production line, with D2 proportions of 25 %, 50 %, and 75 % by weight, denoted as D2/D5 (25/75), D2/D5 (50/50), and D2/D5 (75/25). Blend densities were theoretically predicted by inverse-additive mixing rule as 0.9438 g/cm^3 for D2/D5 (25/75), 0.9467 g/cm^3 for D2/D5 (50/50) and 0.9561 g/cm^3 for D2/D5 (25/75).

2.4. Characterization techniques

Multiple characterization techniques and permeability experiments were conducted to investigate the oxygen permeability behaviour of blown and lab-scale oriented MDO-PE films. For quantifying the oxygen permeability coefficient of randomly oriented or non-uniaxially oriented materials, blown films were selected instead of compression-molded base sheets (used to produce lab-scale MDO films). This choice was made due to the high thickness of the compression-molded base sheets (approximately 550 microns), which made them challenging to use with the oxygen barrier analysis apparatus. In contrast, blown films, with a comparatively lower thickness of about 50 microns (exact value of thickness with standard deviation presented in Table S1 in supplementary information, were more suitable for the experimental setup. Thickness data with standard deviation for lab-scale MDO films used in oxygen barrier analysis is presented in Table S2 in supplementary information.

The various characterization techniques used for the analysis are detailed as follows:

2.4.1. Differential scanning calorimetry (DSC)

Thermal analysis was conducted using a DSC Q2000 instrument from TA Instruments. Samples weighing approximately 5–10 mg, were placed in a closed aluminium pan and subjected to a heat-cool-heat cycle from 0 to 200 °C at a rate of 10 °C/min under a nitrogen atmosphere. Three measurements were taken for each sample. The degree of crystallinity X_{DSC} was calculated using Eq. 1.

$$X_{DSC} = \frac{\Delta H_m}{\Delta H_m} * 100 \quad (1)$$

Where ΔH_m is the melting enthalpy, and ΔH_m is the melting enthalpy of 100 % crystalline PE, i.e., 293 J/g (Blaine, 2010).

2.4.2. X-Ray diffraction

Microstructural analysis of the samples was conducted using X-ray diffraction (XRD) technique: wide-angle X-ray scattering (WAXS). Data were collected at the Advanced Photon Source (APS), DND-CAT, 5-ID-D beamline at Argonne National Laboratory (Lemont, IL, USA), using the APS Undulator A as the X-ray source with an X-ray energy of 17 keV (λ =

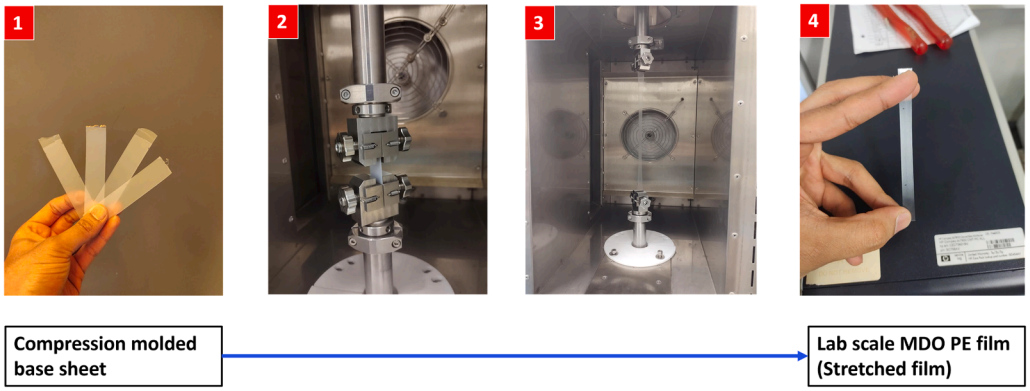

Fig. 1. Pictorial representation of step-wise lab-scale MDO stretching process.

0.7293 Å). Data analysis was performed using the Jade software. The crystallite size was calculated from the full width at half maximum (β) of the crystalline peak using Debye-Scherrer's equation (Eq. 2).

$$L_{hkl} = \frac{K\lambda}{\beta * \cos\theta} \tag{2}$$

Where L_{hkl} is crystallite dimension (in Å) along the direction perpendicular to the crystallographic plane *hkl*, β is the full width of the diffraction line at half maximum of peak related to the crystallographic plane *hkl* in radians, θ is the diffraction angle (Bragg's angle) of the *hkl* reflection, λ is the wavelength of X-ray, and K is the Scherrer constant with value of 0.89. Five measurements were taken for each sample.

In uniaxial orientation, the distribution functions of the chain segment orientations are defined using a series of orthogonal spherical harmonic functions. Crystalline orientation is characterized by calculating the average squared cosine values, which represent the average orientation of the normal to the crystalline plane relative to each reference axis. Herman's orientation function, the second harmonic orientation function, is expressed using Eq. 3 (Prasad et al., 2001).

$$f = \frac{3\langle\cos^2\varphi_{hkl,z}\rangle - 1}{2} \tag{3}$$

Where $\varphi_{hkl,z}$ is the angle between the chain axis and a reference axis z, which is the draw direction (DD). $\langle\cos^2\varphi_{hkl,z}\rangle$ is calculated from the scattering intensity $I(\varphi)$ by integrating over the azimuthal angle ϕ as given in Eq. 4.

$$\langle\cos^2\varphi_{hkl,z}\rangle = \frac{\int_0^{\pi/2} I(\varphi)\sin\varphi\cos^2\varphi d\varphi}{\int_0^{\pi/2} I(\varphi)\sin\varphi d\varphi} \tag{4}$$

The value of f is 1 (φ =0) for the perfect draw direction orientation, −1/2 (φ =90) for chains aligned normally to the draw direction, and 0 for a perfect random orientation. Five measurements were taken for each sample for the calculation of crystallite dimension and apparent crystallinity.

2.4.3. Permeability

Oxygen permeability of the films was measured using ASTM D3985 method by a MOCON OX-TRAN 702 instrument using the equal pressure method at 23°C, 1 atm pressure and 0 % relative humidity (RH) on both sides of the material (Figure S2 in supplementary information). Samples were masked with aluminium covers exposing only about 3 cm^2 area for blown films and about 1 cm^2 area for lab scale MDO-PE films for the passage for permeant. Air containing approximately 20.9 % of oxygen was passed on one side of the film inside the unit cell as test gas and the formier gas (95 % nitrogen + 5 % hydrogen) as a carrier gas on the other side of the film inside the unit cell. All test measurements were recalculated to 100 % oxygen as test gas. Owing to the time-intensive nature of the experiment and the availability of the permeability apparatus, one repeat measurement was made for each sample. The repeat measurements showed very close agreement with the initial values, indicating good reproducibility (Table S5, supplementary information).

The Permeability coefficient (P) is normalised to a constant thickness at given temperature and pressure (Morris, 2017). Hence P was quantified to negate the effect of thickness on transmission of oxygen. The permeability coefficient is given by the following Eq. 5.

$$P = \frac{(quantity\ of\ permeant)(film\ thickness)}{(area)(time)(pressure\ drop\ across\ film)} \tag{5}$$

3. Results and discussions

As mentioned in Section 2, the objective of the experiments was to quantify whether the microstructural orientation of uniaxially stretched lab-scale MDO films, prepared by stretching compression-molded base sheets, would lead to an enhancement in the oxygen barrier properties compared to randomly oriented blown PE films of same material.

3.1. Crystallinity data from DSC analysis

The overall crystallinity data obtained from DSC analysis was evaluated for the compression-molded base sheets, their corresponding lab-scale MDO films. The crystallinity was also evaluated for blown films of the five base resins. Crystallinity is a key factor influencing oxygen barrier properties, as polymer crystals act as impermeable barriers to the passage of permeant molecules, with diffusion occurring primarily through the amorphous regions (Ansari et al., 2025; Breese & Beaucage, 2005; Chatterjee et al., 2014; Paulos & Thomas, 1980; Safandowska et al., 2022; Sha & Harrison, 1992). Fig. 2 compares DSC thermograms (1st heat cycle) of compression molded base sheets of all five resins along with their peak melting temperature (T_m). The enthalpy of melting and peak melting temperature increased with increase in resin density, which implies an increase in percent crystallinity and crystallite size of the base sheets as density increases.

3.1.1. Crystallinity comparison of MDO films (after stretching) and their preform compression molded base sheets (before stretching)

Fig. 3 compares overall crystallinity of the compression molded base sheet of all five base resins D1, D2, D3, and D4 and three blends of D2/D5 with crystallinity of MDO films obtained by the lab-scale MDO process as a function of base-resin density.

The density of the blends was calculated theoretically using an inverse-additive mixing rule. The stretching process might have altered the densities of stretched films to a small amount, but for the comparative analysis, results of the stretched films are presented in terms of the densities of the base sheets. Lowest density resin D1 only shows about a 4 % increase in crystallinity whereas higher-density resins D4 and D2/D5 (25/75) film showed as much as about 10 % increase after stretching. This result is also an indication of in general higher disintegration and fibrillation in the initial crystalline structure and strain-induced orientation and crystallization of the amorphous regions of base sheets made from higher-density resin during stretching at the used orientation temperature. This trend is further supported by the higher slope value of approximately 818 observed for the MDO films, compared to about 692 for the compression-molded base sheets, as obtained from the linear regressions shown in Fig. 3.

During the first DSC heating cycle, the prior mechano-thermal history of the samples was erased through melting, thereby eliminating the effects of processing-induced orientation and crystallization in both compression-molded base sheets and their MDO films. Consequently, the second DSC heating cycle represents the intrinsic thermal behavior of the material after controlled cooling under identical conditions. Under these conditions, the DSC thermograms of the compression-molded base sheets and the lab-scale MDO films were highly similar in the second heating cycle, exhibiting similar melting enthalpy and crystallinity values (Table S3, Supplementary Information). These findings therefore confirm that MDO processing induces additional crystallinity in the MDO-PE films relative to their preform compression-molded base sheets as indicated by DSC first heat cycle data.

3.1.2. Crystallinity comparison of MDO films and blown films of five base PE resins used in the study

Fig. 4 presents a comparison of the overall crystallinity between lab-scale MDO films and blown films produced from five base resins. The data demonstrates enhanced overall crystallinity of the lab-scale MDO-PE films of all five base resins compared to the blown films from same materials. Additionally, the crystallinity of the compression-molded base sheets of the five base resins was found to be quite similar to that of the blown films of base resins.

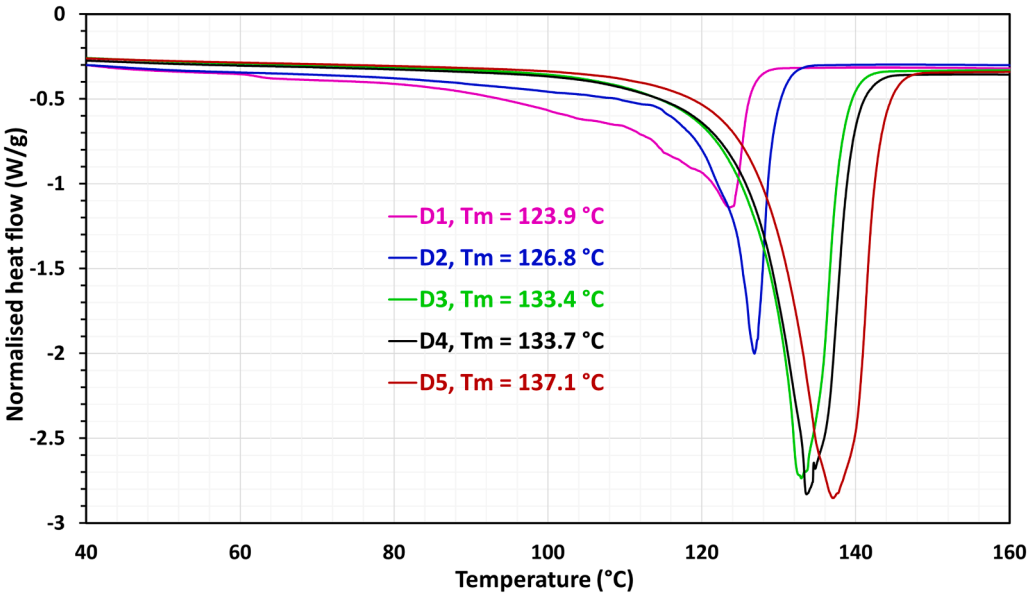

Fig. 2. DSC melting curves obtained during 1st heat cycle for compression molded base sheets from all 5 base resins along with their peak melting temperature (T_m).

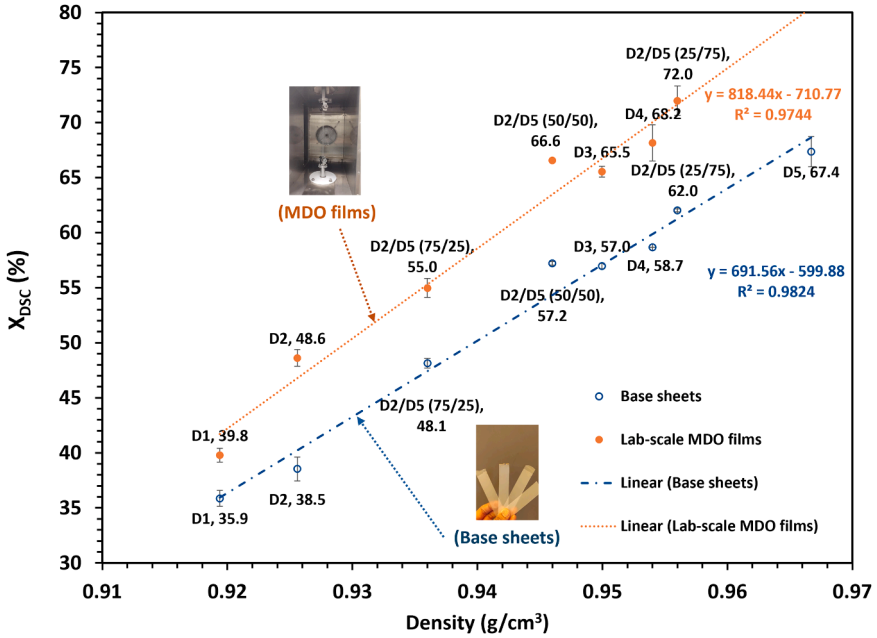

Fig. 3. Degree of crystallinity (X_{DSC}) (DSC, 1st run) of all five base sheets and MDO films as a function of base resin density. (Note 1: D5 could not be stretched to the length draw ratio of 7 during MDO) (Note 2: The linear curves are plotted by fitting the points into a linear equation).

In blown film extrusion, the BUR and DDR are key processing parameters that control film thinning and molecular orientation, with BUR primarily influencing transverse-direction orientation and DDR governing machine-direction orientation. Crystallinity in blown films is primarily established during melt cooling, during which polymer chains crystallize directly from the molten state under the combined influence of melt flow, cooling rate, and extensional deformation. The relatively moderate and comparable BUR (2.31) and DDR (3.15) employed in this study were therefore not expected to induce strong preferential molecular orientation in either direction, a conclusion supported by the WAXS results presented in the latter section. In contrast, the MDO process involves stretching the film in a semi-solid state at temperatures below the polymer's peak melting temperature, leading to a fundamentally different microstructural evolution characterized by lamellar fragmentation, fibrillation, and additional strain-induced crystallization within the amorphous phase. Consequently, MDO processing resulted in enhanced overall crystallinity compared to blown films.

3.2. WAXS analysis of microstructural evolution during lab-scale MDO stretching (MDO films and their preform compression molded base sheets)

The WAXS results offered a more comprehensive understanding of the structural evolution during lab-scale MDO operations by enabling the analysis of microstructural data such as crystallite dimensions, before and after the stretching process. Results for D5 were not obtained as D5 base sheet could not be stretched to the length draw ratio of 7 due to its extremely high density and crystallinity as compared to other resins and blends. Due to the high fraction of crystalline phase, its

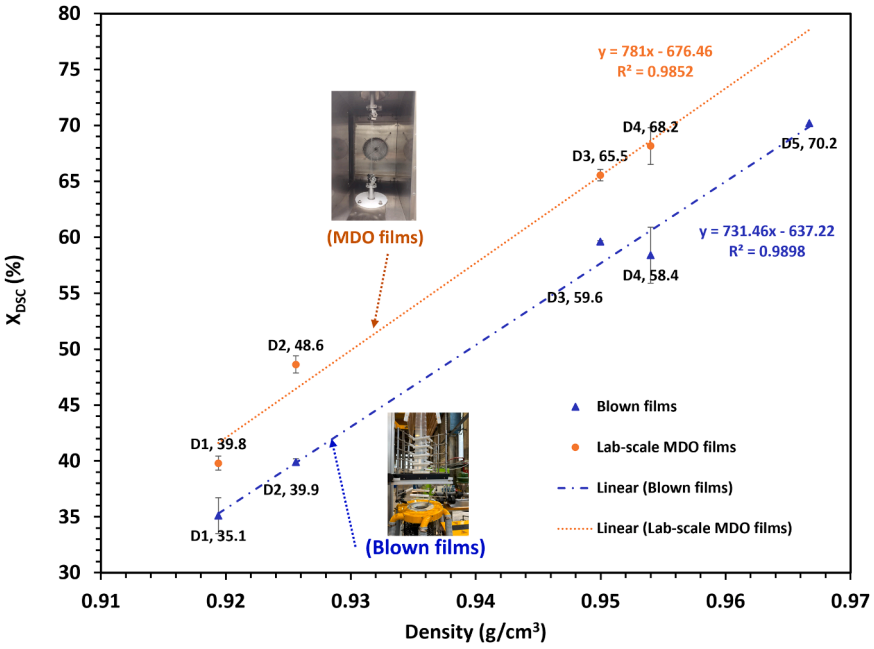

Fig. 4. Degree of crystallinity (X_{DSC}) of all five blown films and lab-scale MDO films as a function of base resin density. (Calculated from enthalpy data from DSC, 1st run). (Note: D5 could not be stretched to the length draw ratio of 7).

microstructure showed extreme fibrillation and necking during stretching at the used specific orientation temperature and thus ultimately broke off under tensile load.

It was anticipated that the average crystallite dimension would decrease during the drawing process for films derived from high-density resins with larger crystallite sizes. This expectation was confirmed by the observed reduction in average crystallite dimension for D3 and D4 films after drawing, as evidenced from the Fig. 5.

Interestingly the same was not observed for the films made from low-density resins D1 and D2. The DSC (Fig. 2) melting curves during 1st heat cycle indicated that partial melting of crystalline phase was relatively higher for these resins as fixed orientation temperature of 110 °C was closer to the peak melting point of these resins as compared to higher density resins D3, D4, and D5. This possibly might have helped to retain similar (in case of D2) or even larger (in case of D1) crystallite size after the drawing process at the fixed length draw ratio of 7, as its microstructure was relatively more mobile and thus less disintegrated and fibrillated under tensile load.

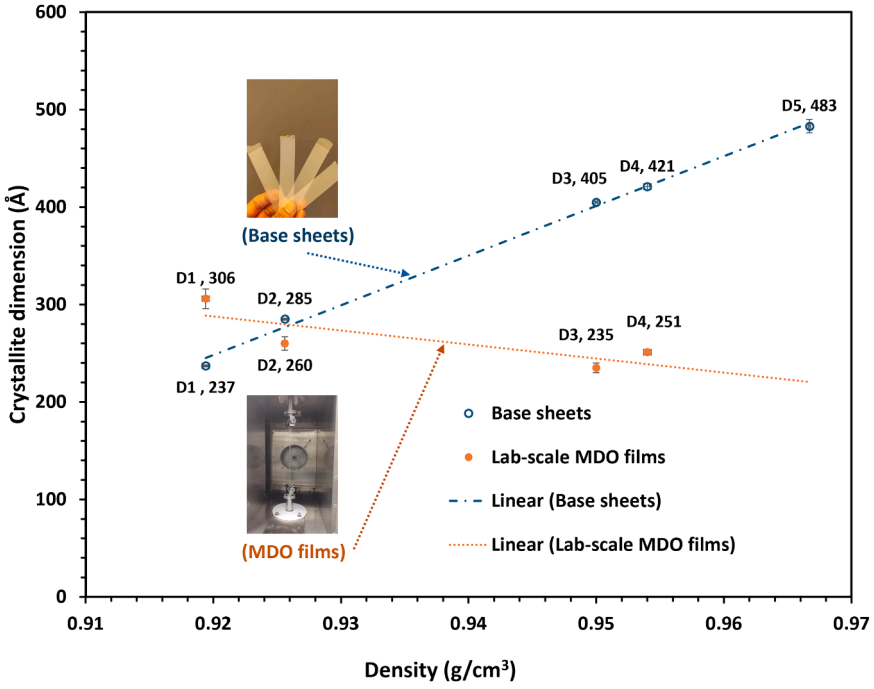

Fig. 5. Crystallite dimension, L (110) for the compression molded base sheets (before stretching) and their counterpart lab-scale MDO films (after stretching) of 5 base resins as a function of base resin density. (Note: D5 could not be stretched to the process draw ratio of 7).

3.3. Analysis of the crystal orientations from WAXS analysis for base sheets, MDO films and blown films

The 2D WAXS patterns gave insight on the orientation of the microstructure of base sheets and MDO films as represented by Fig. 6. The orientation was quantified using Herman's orientation functions from WAXS data.

Polyethylene (PE) films with an orthorhombic crystal structure typically exhibit strong scattering from the [110] and [200] reflection planes (with the latter corresponding to the a-axis) and relatively weaker scattering from the [020] plane (corresponding to the b-axis). The [002] reflection plane (c-axis) is generally not observed. To assess the orientation of the crystalline phase, an intensity profile is obtained by plotting the intensity versus azimuthal angle for a user-defined annular region, focusing on the [200] and [020] reflections. The intensity at a given azimuthal angle is dependent on the quantity of crystallographic planes oriented appropriately to permit diffraction at that angle.

In the 2D wide-angle X-ray scattering (WAXS) patterns (Fig. 6a) of compression-molded base sheets, intense and uniform reflections from the [110] and [200] planes of the orthorhombic unit cell are observed, along with weaker reflections from other planes. This pattern suggests a

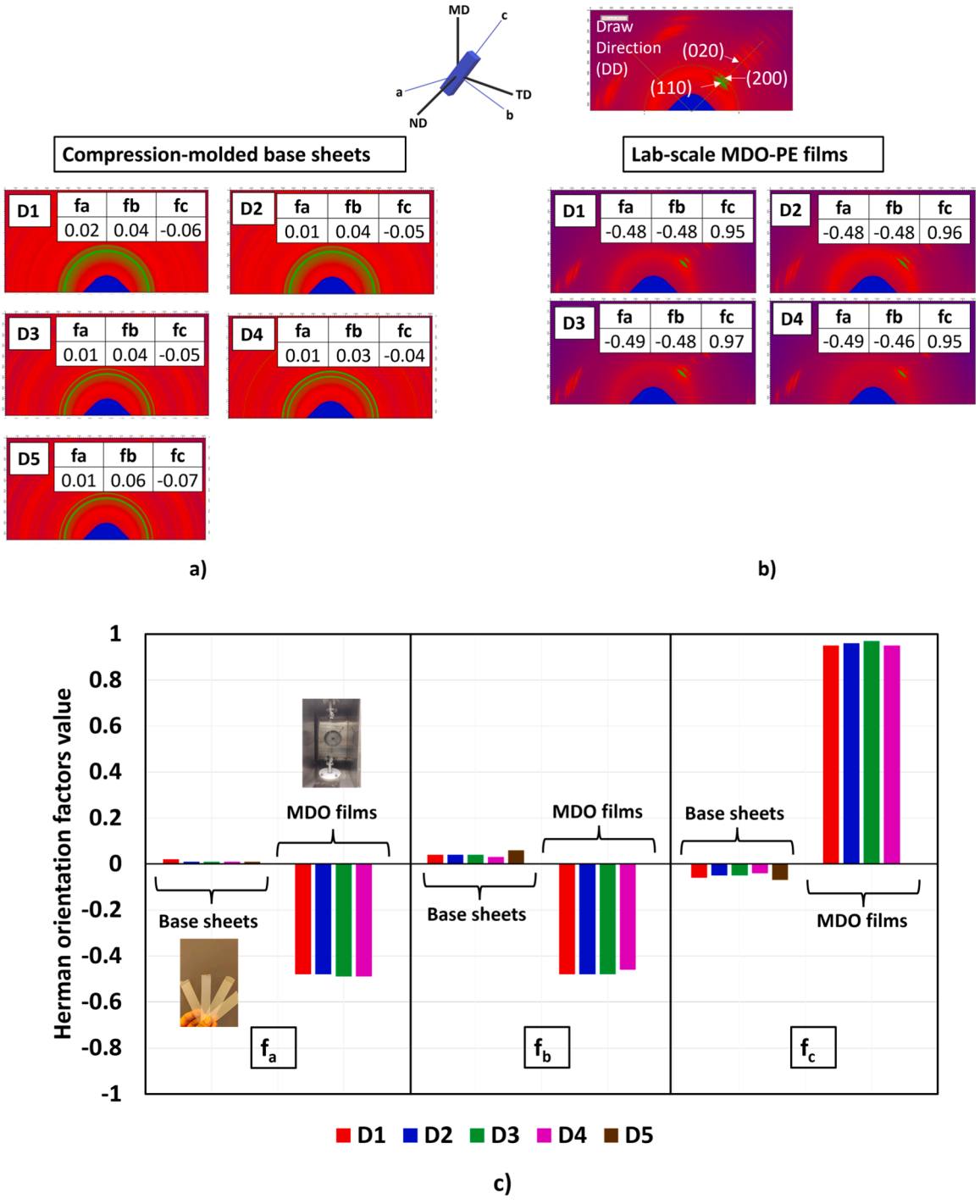

Fig. 6. 2D WAXS patterns for **a)** compression molded base sheets of all 5 base PE resins (D1, D2, D3, D4 and D5) and **b)** for lab-scale MDO films (D1, D2, D3 and D4) along with their Herman orientation factors. **c)** bar graph comparison of Herman orientation factors (f_a, f_b and f_c) for base sheets and MDO films.

random orientation of the microstructure. As expected, no strong microstructural orientation was detected across all samples, a finding further supported by the quantification using Herman's orientation functions (illustrated in Fig. 6a). The orientation factors fa, fb, and fc for the orthorhombic crystallographic axes a, b, and c, respectively, are all close to 0, indicating an isotropic crystalline structure.

Herman orientation factors obtained for PE blown films (Table S4, supplementary information) were in between −0.24–0.22 in all three axes. Consequently, no pronounced crystal orientation along either the machine or transverse direction was detected, indicating predominantly random orientation.

In contrast, the lab-scale machine-direction oriented (MDO) films (Fig. 6b) exhibited a pronounced crystalline orientation, as evidenced by the strongly defined and intense equatorial diffraction arcs corresponding to the [110], [200], and [020] planes. The orientation factor f_c for the crystallographic c-axis was nearly 1, indicating an almost perfect alignment of the c-axis with the draw direction.

Quantifying the orientation of the amorphous regions using 2D diffraction patterns is also possible; however, this was challenging in this study due to the strong crystalline scattering peaks superimposed on the amorphous halo. Nonetheless, it is expected that the tensile forces applied during the MDO process, particularly at the chosen orientation temperature, would also induce significant orientation in the amorphous regions toward the machine direction. This effect is likely more pronounced in higher-density base sheets due to the relatively lower proportion of amorphous regions, which facilitates easier disentanglement and orientation under the applied stretching load.

3.4. Oxygen permeability analysis

For quantifying the oxygen permeability coefficient of randomly oriented or non-uniaxially oriented materials, blown films were selected instead of compression-molded base sheets (used to produce lab-scale MDO films). This choice was due to the high thickness of the compression-molded base sheets (approximately 550 microns), which made them challenging to use with the apparatus. In contrast, blown films, with a comparatively lower thickness of about 50 microns (exact value of thickness with standard deviation presented in Table S1 in supplementary information), were more suitable for the experimental setup.

Fig. 7 presents the analysis of permeability coefficient data to compare the oxygen permeability between lab-scale MDO films and blown films made from base resins and selected blends.

In semi-crystalline polymers, polymer crystals serve as impermeable barriers, with small molecules diffusing primarily through the amorphous regions. Consequently, an increase in overall crystallinity or film density is expected to result in reduced permeability. This relationship is corroborated by the data presented in Fig. 7, where decrease in permeability is observed as density increases for both blown and lab-scale MDO films. This decrease in oxygen permeability with increasing PE density is in line with the previous work from Alter (Alter, 1962).

Interestingly from Fig. 7, it was observed that MDO orientation did not always improved oxygen barrier in lab-scale MDO films compared to blown films. Specifically, in lower-density films, such as D1 and D2, oxygen permeability was higher in lab-scale MDO films. However, the trendline indicates that after surpassing a certain density (0.947 g/cm^3 for D2/D5 (50/50)), the oxygen permeability in lab-scale MDO films at the fixed MDO length draw ratio of 7 and orientation temperature of 110 °C decreased relative to the blown films. It is further acknowledged that incorporating additional data points could refine the trendline and provide a more comprehensive understanding of the impact of orientation on permeability coefficients, which presents an opportunity for future investigation.

It is important to note that permeability in the MDO process is also influenced by the draw ratio and orientation temperature, with permeability likely to be expected to decrease as the draw ratio increases and orientation temperature decreases as mentioned in literature (Breese & Beaucage, 2005; Paulos & Thomas, 1980). In this study, the

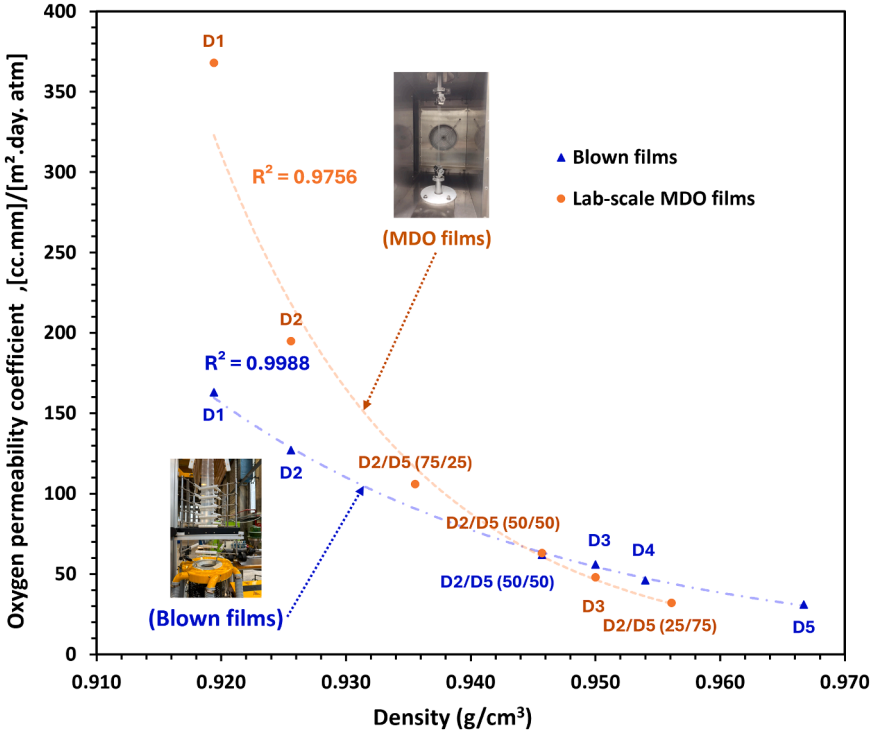

Fig. 7. Oxygen permeability coefficient (each sample measurement repeated once for accuracy) for lab-scale MDO films and blown films made from base resins and selected blends as a function of base resin density with data points fitted for an exponential fit indicated by dashed trendlines. (Note: In case of blown films of blends, oxygen permeability coefficient of only one blend i.e. D2/D5 (50/50) was measured. Further lab-scale MDO film sample of D4 failed during measurement giving an outlier value.).

lab-scale MDO operation was conducted using a fixed draw ratio and orientation temperature. Therefore, it is highly likely that varying the draw ratio and orientation temperature in the lab-scale MDO process could yield different permeability results for the same material.

Paulos and Thomas (1980), in their investigation of the effect of post drawing on gas permeability in blown polyethylene films, reported that a higher degree of sample orientation is preserved at lower orientation temperatures (or less partially melted microstructure) during post drawing. They attributed the significant reduction in the films transport properties primarily to the increased orientation of the amorphous phase. Similarly, Nakayama and Katsuna (Nakayama & Kanetsuna, 1975) demonstrated a similar relationship between the orientation of the amorphous phase and the orientation temperature.

Fig. 4 also presented that lab-scale MDO films exhibit higher overall crystallinity compared to blown films of similar resins. However, despite this increased crystallinity, the D1 and D2 lab-scale MDO films displayed higher oxygen permeability than their blown film counterparts. These findings indicate that merely increasing overall crystallinity after MDO does not necessarily enhance the gas permeability barrier of an oriented polymer film. The orientation and geometric configuration of both crystalline and amorphous regions after MDO operation also plays a crucial role in determining barrier properties of the oriented polymer film (Breese & Beaucage, 2005; Paulos & Thomas, 1980).

As presented in the DSC percent crystallinity comparison of base sheets and their MDO films in Fig. 3, the increase in overall crystallinity is minimal for the lowest-density resin, D1, compared to the other resins. This suggests that the extensive partial melting of the crystalline phase at the used orientation temperature did not significantly produce strong amorphous orientation during MDO stretching. Consequently, this is reflected in the oxygen permeability properties of D1, which increased after stretching and orientation compared to its blown film. As resin density increases, the disintegration and fibrillation of the crystalline phase become more pronounced due to the relatively lower extent of partial melting of the crystalline microstructure at the used fixed orientation temperature. This, in turn facilitates stronger orientation and crystallization of the amorphous regions. The resulting decrease in oxygen permeability in lab-scale MDO films compared to blown films with increasing density is indicative of these relatively stronger amorphous orientations in higher density lab-scale MDO films. Lasoski and Cobbs (Lasoski & Cobbs, 1959), in their investigation on comparing moisture permeability of oriented and non-oriented PET films at similar density also observed lesser permeability for oriented films and further suggested that the “locking-in” of orientation by the ensuing crystallization permits the orientation to have an effect additive to that of crystallinity in reducing the permeability of a film.

Another factor contributing to the reduced oxygen barrier properties observed after orientation, particularly in low-density lab-scale MDO films D1 and D2, may be related to the geometric configuration of the lamellae. This phenomenon is supported by the findings of Breese *et al.* (Breese & Beaucage, 2005), who investigated the impact of MDO on the moisture and oxygen barrier properties of HMW (high molecular weight)-PE films. Their study revealed that MDO films produced from lower density materials exhibited increased moisture and oxygen transmission rates. They attributed this to the lamellae's (thin plate-like crystalline structural component in semi-crystalline polymers that forms during crystallization process by back-and-forth orderly folding of polymer chains) arrangement at low to moderate draw ratios, where the lamellae are aligned nearly parallel to each other, thereby exposing inter- and intra-lamellar stack voids that facilitate the permeation of moisture and oxygen through the films. However, no conclusive evidence was found to support this argumentation in the experiments.

The oxygen permeability of conventionally used outer polymer films for multilayer flexible packaging, such as PET and PA, typically ranges from 1 to 5 cc.mm/m^2.day.atm for PET and 0.1–1 cc.mm/m^2.day.atm for PA at 0 % RH and 23°C, as reported in the literature (Lange & Wyser, 2003). These values are significantly lower than the lowest permeability observed in this study’s measurements for lab-scale MDO-PE films, which was approximately 30–40 cc.mm/m^2.day.atm at the same temperature and relative humidity.

Hence, it is suggested that while MDO-PE films can enhance oxygen barrier properties under certain conditions, they may still require an additional oxygen barrier layer for high-end packaging applications. This additional barrier, potentially in the form of ultra-thin coatings or high-performance barrier films, should also be compatible with mechanical recycling processes for mono-material PE-based multi-layer flexible packaging designed for high oxygen barrier requirements. Few companies and consortia, such as The Circular Economy for Flexible Packaging (CEFLEX) (DESIGNING FOR A CIRCULAR ECONOMY An introduction, 2020), which develop guidelines for the recycling of flexible packaging, accept the inclusion of strong oxygen barrier layers like ethylene vinyl alcohol (EVOH), provided these materials do not exceed 5 % by weight of the total packaging structure. This threshold ensures that the final quality of the recyclate is not compromised and that the packaging structure remains classified as mono-material flexible packaging.

4. Concluding remarks

This study investigated the effects of uniaxial orientation on the oxygen barrier property of polyethylene films for mono-material PE based multi-layer flexible packaging designed to support mechanical recycling.

The experiments evaluated the oxygen barrier properties of lab-scale MDO-PE films against randomly oriented PE blown films, demonstrating that higher-density MDO films exhibited improved barrier performance due to increased overall crystallinity and micro-structural orientation. In contrast, lower-density MDO films showed increased oxygen permeability after orientation, attributed to higher microstructural partial melting and possibly limited amorphous phase orientation during MDO. The results highlight the importance of optimizing resin density at constant MDO process parameters to achieve optimal oxygen barrier properties in MDO-PE films. While MDO operation demonstrated the potential to improve oxygen barrier properties of PE films at certain resin and process parameters, the oxygen permeability of MDO-PE films remained higher than that of conventional barrier materials like PET and PA, underscoring the need for supplementary oxygen barrier layers for high-performance applications which must be compatible with mechanical recycling pf PE based mono-material flexible packaging. While this study focused on the oxygen permeability of relatively thinner PE blown and MDO films, measuring the permeability of relatively thicker precursor compression-molded PE base sheets or films used for MDO operation would provide additional insight into the influence of MDO processing and orientation on oxygen barrier properties. This presents an interesting avenue for future research.

CRediT authorship contribution statement

Jaap den Doelder: Writing – review & editing, Supervision, Resources, Methodology, Funding acquisition, Conceptualization. **Peter Ragaert:** Writing – review & editing, Visualization, Supervision, Resources, Methodology, Conceptualization. **Roos Peeters:** Writing – review & editing, Resources, Methodology, Conceptualization. **Dixit Guleria:** Writing – original draft, Visualization, Methodology, Investigation, Formal analysis, Data curation, Conceptualization. **Dimitri Adons:** Methodology, Investigation, Formal analysis, Data curation.

Declaration of Competing Interest

The authors declare that they have no known competing financial interests or personal relationships that could have appeared to influence the work reported in this paper.

Acknowledgements

This work has been performed in the framework of the C-PlaNeT (Circular Plastics Network for Training) project which has received funding from the European Union's Horizon 2020 research and innovation program under the Marie Sklodowska-Curie grant agreement No 859885.

Appendix A. Supporting information

Supplementary data associated with this article can be found in the online version at doi:10.1016/j.fpsl.2026.101711.

Data availability

Data will be made available on request.

References

Alter, H. (1962). A critical investigation of polyethylene gas permeability. *Journal of Polymer Science, 57*(165), 925–935. https://doi.org/10.1002/pol.1962.1205716572

Ansari, J. R., Park, K., Sadeghi, K., & Seo, J. (2025). Preparation of MoS2 modified with carbon quantum dots and its application to extremely high oxygen-barrier nanocomposite films for packaging. *Food Packaging and Shelf Life, 49*, Article 101504. https://doi.org/10.1016/j.fpsl.2025.101504

Ayuso, C. F., Agüero, A. A., Hernández, J. A. P., Santoyo, A. B., & Gómez, E. G. (2017). High oxygen barrier polyethylene films. *Polymers and Polymer Composites, 25*(8), 571–582. https://doi.org/10.1177/096739111702500802

Barlow, C. Y., & Morgan, D. C. (2013). Polymer film packaging for food: An environmental assessment. *Resources, Conservation and Recycling, 78*, 74–80. https://doi.org/10.1016/j.resconrec.2013.07.003

Blaine, R. L. (2010). Determination of polymer crystallinity by DSC. *Therm. Anal. TA Instruments* (pp. 1–3). ⟨https://www.scirp.org/reference/referencespapers?referenceid=1920439⟩, 109 Lukens Drive, New Castle DE 19720, USA.

Breese, R., & Beaucage, G. (2005). Effects of machine direction orientation (MDO) on the moisture and oxygen barrier properties of HMW-PE films. *TAPPI European PLACE Conference, 2005*. ⟨https://citeseerx.ist.psu.edu/document?repid=rep1&type=pdf&doi=98756ceb8d83a156b6e0307dea67c0b15236cf3d⟩.

Carullo, D., Casson, A., Rovera, C., Ghaani, M., Bellesia, T., Guidetti, R., & Farris, S. (2023). Testing a coated PE-based mono-material for food packaging applications: An in-depth performance comparison with conventional multi-layer configurations. *Food Packaging and Shelf Life, 39*, Article 101143. https://doi.org/10.1016/j.fpsl.2023.101143

Chatterjee, T., Patel, R., Garnett, J., Paradkar, R., Ge, S., Liu, L., Forziati, K. T., & Shah, N. (2014). Machine direction orientation of high density polyethylene (HDPE): Barrier and optical properties. *Polymer, 55*(16), 4102–4115. https://doi.org/10.1016/j.polymer.2014.06.029

Chen, C., Wang, L., Shams Es-haghi, S., Tajvidi, M., Wang, J., & Gardner, D. J. (2024). Biodegradable and recyclable bio-based laminated films of poly (lactic acid) and cellulose nanocrystals for food barrier packaging. *Food Packaging and Shelf Life, 42*, Article 101244. https://doi.org/10.1016/j.fpsl.2024.101244

Comyn, J. (2005). What are adhesives and sealants and how do they work? In R. D. Adams (Ed.), *Adhesive Bonding, 2* pp. 23–51) Woodhead Publishing. https://doi.org/10.1533/9781845690755.1.23.

DeMeuse, M. T. (2011). Equipment design and requirements of biaxially stretched films. *Biaxial stretching of film* (pp. 14–26). Elsevier. https://doi.org/10.1533/9780857092953.1.14

DESIGNING FOR A CIRCULAR ECONOMY An introduction. (2020). ⟨https://guidelines.ceflex.eu/assets/public_docs/D4ACE_guidelines_An_Introduction.pdf⟩.

Dilkes-Hoffman, L. S., Lane, J. L., Grant, T., Pratt, S., Lant, P. A., & Laycock, B. (2018). Environmental impact of biodegradable food packaging when considering food waste. *Journal of Cleaner Production, 180*, 325–334. https://doi.org/10.1016/j.jclepro.2018.01.169

Elias, M. B., Machado, R., & Canevarolo, S. V. (2000). Thermal and Dynamic-Mechanical Characterization of Uni- and Biaxially Oriented Polypropylene Films. *Journal of Thermal Analysis and Calorimetry, 59*(1), 143–155. https://doi.org/10.1023/A:1010187913049

Faraca, G., & Astrup, T. (2019). Plastic waste from recycling centres: Characterisation and evaluation of plastic recyclability. *Waste Management, 95*, 388–398. https://doi.org/10.1016/j.wasman.2019.06.038

Guerritore, M., Olivieri, F., Castaldo, R., Avolio, R., Cocca, M., Errico, M. E., Galdi, M. R., Carfagna, C., & Gentile, G. (2022). Recyclable-by-design mono-material flexible packaging with high barrier properties realized through graphene hybrid coatings. *Resources, Conservation and Recycling, 179*. https://doi.org/10.1016/j.resconrec.2021.106126

Guleria, D., Debrie, S., Ge, S., Vervoort, S., den Doelder, J., Cardon, L., & Edeleva, M. (2025). Assessing mechanical recyclability of blown films and integration of PCR for high modulus uniaxially drawn PE film application. *Polymer Degradation and Stability, 240*, Article 111458. https://doi.org/10.1016/j.polymdegradstab.2025.111458

Guleria, D., Edeleva, M., Vervoort, S., Ge, S., den Doelder, J., & Cardon, L. (2024). Impact of molecular architecture and draw ratio on enhancement of targeted mechanical properties of machine direction oriented polyethylene films produced after blown film extrusion, 87560879241293390 *Journal of Plastic Film Sheeting*. https://doi.org/10.1177/87560879241293392.

Guleria, D., Ge, S., Cardon, L., Vervoort, S., & den Doelder, J. (2024). Impact of resin density and short-chain branching distribution on structural evolution and enhancement of tensile modulus of MDO-PE films. *Polymer Testing.* , Article 108560. https://doi.org/10.1016/j.polymertesting.2024.108560

Guzman-Puyol, S., Benítez, J. J., & Heredia-Guerrero, J. A. (2022). Transparency of polymeric food packaging materials. *Food Research International, 161*, Article 111792. https://doi.org/10.1016/j.foodres.2022.111792

Hatfield, Eric, Tate, Richard, Williams, Kelly, & Todd, William (2002). New MDO Medium Molecular Weight High Density Polyethylene Films. *Journal of Plastic Film Sheeting, 18*(2), 117–127. https://doi.org/10.1177/8756087902018002006

Jost, V. (2018). Packaging related properties of commercially available biopolymers - An overview of the status quo. *Express Polymer Letters, 12*(5), 429–435. https://doi.org/10.3144/expresspolymlett.2018.36

Kaiser, K., Schmid, M., & Schlummer, M. (2018). Recycling of polymer-based multilayer packaging: A review (MDPI AG) *In Recycling, 3*(1). https://doi.org/10.3390/recycling3010001.

Lange, J., & Wyser, Y. (2003). Recent innovations in barrier technologies for plastic packaging—A review. *Packaging Technology and Science, 16*(4), 149–158. https://doi.org/10.1002/pts.621

Lasoski, S. W., Jr., & Cobbs, W. H., Jr. (1959). Moisture permeability of polymers. I. Role of crystallinity and orientation. *Journal of Polymer Science, 36*(130), 21–33. https://doi.org/10.1002/pol.1959.1203613003

Lazić, V., Budinski-Simendić, J., Gvozdenović, J., & Simendić, B. (2010). Barrier properties of coated and laminated polyolefin films for food packaging. *Acta Physica Polonica A, 117*(5), 855–858.

Ma, W., Lu, Y., Liu, Y., Li, D., & Li, L. (2024). Enhanced permeability of ZnO/PE films by stretching and its application in Pakchoi preservation. *Food Packaging and Shelf Life, 43*, Article 101296. https://doi.org/10.1016/j.fpsl.2024.101296

Ma, Y. (2018). Changing Tetra Pak: From waste to resource. *Science Progress, 101*(2), 161–170. https://doi.org/10.3184/003685018x15215434299329

Morris, B. A. (2017). Barrier. *The science and technology of flexible packaging* (pp. 259–308). Elsevier. https://doi.org/10.1016/B978-0-323-24273-8.00008-3

Nakayama, K., & Kanetsuna, H. (1975). Hydrostatic extrusion of solid polymers. *Journal of Materials Science, 10*(7), 1105–1118. https://doi.org/10.1007/BF00541391

Paul, M., Morris, B., Weinhold, J., & Hausmann, K. (2022). The effect of stretching and tie layer composition on adhesion strength of multi-layered films. *Journal of Plastic Film and Sheeting, 38*(3), 351–368. https://doi.org/10.1177/87560879211063475

Paulos, J. P., & Thomas, E. L. (1980). Effect of postdrawing on the permeability of gases in blown polyethylene film. *Journal of Applied Polymer Science, 25*(1), 15–23. https://doi.org/10.1002/app.1980.070250102

Prasad, A., Shroff, R., Rane, S., & Beaucage, G. (2001). Morphological study of HDPE blown films by SAXS, SEM and TEM: A relationship between the melt elasticity parameter and lamellae orientation. *Polymer, 42*(7), 3103–3113. https://doi.org/10.1016/S0032-3861(00)00612-1

Qasim, U., Osman, A. I., Al-Muhtaseb, A. H., Farrell, C., Al-Abri, M., Ali, M., Vo, D.-V. N., Jamil, F., & Rooney, D. W. (2021). Renewable cellulosic nanocomposites for food packaging to avoid fossil fuel plastic pollution: A review. *Environmental Chemistry Letters, 19*(1), 613–641. https://doi.org/10.1007/s10311-020-01090-x

Risch, S. J. (2009). Food packaging history and innovations. *Journal of Agricultural and Food Chemistry, 57*(18), 8089–8092. https://doi.org/10.1021/jf900040r

Safandowska, M., Makarewicz, C., Rozanski, A., & Idczak, R. (2022). Barrier properties of semicrystalline polylactide: The role of the density of the amorphous regions. *Macromolecules, 55*(22), 10077–10089. https://doi.org/10.1021/acs.macromol.2c01490

Sha, H., & Harrison, I. R. (1992). CO2 permeability and amorphous fractional free-volume in uniaxially drawn HDPE. *Journal of Polymer Science Part B: Polymer Physics, 30*(8), 915–922. https://doi.org/10.1002/polb.1992.090300814

Soares, C. T. de M., Ek, M., Östmark, E., Gällstedt, M., & Karlsson, S. (2022). Recycling of multi-material multilayer plastic packaging: Current trends and future scenarios. *Resources, Conservation and Recycling, 176*. https://doi.org/10.1016/j.resconrec.2021.105905

Srebrenkoska, V., Gaceva, G. B., Avella, M., Ericco, M. E., & Gentile, G. (2009). Utilization of recycled polypropylene for production of Eco-composites. *Polymer - Plastics Technology and Engineering, 48*(11), 1113–1120. https://doi.org/10.1080/03602550903147247

Tabatabaei, S. H., Carreau, P. J., & Ajji, A. (2009). Structure and properties of MDO stretched polypropylene. *Polymer, 50*(16), 3981–3989. https://doi.org/10.1016/j.polymer.2009.06.059

Tabatabaei, S. H., Parent, L., Cigana, P., Ajji, A., & Carreau, P. J. (2009). Effect of machine direction orientation conditions on properties of HDPE films. *Journal of Plastic Film and Sheeting, 25*(3–4), 235–249. https://doi.org/10.1177/8756087910369423

Thomas, J., Selvin Thomas, P., & Stephen, R. (2024). Improved mechanical, thermal, and barrier properties of halloysite nanotubes and nanocellulose incorporated PVA-PEO films: For food packaging applications. *Food Packaging and Shelf Life, 46*, Article 101373. https://doi.org/10.1016/j.fpsl.2024.101373

Trinh, B. M., Chang, B. P., & Mekonnen, T. H. (2023). The barrier properties of sustainable multiphase and multicomponent packaging materials: A review. *Progress in Materials Science, 133*, Article 101071. https://doi.org/10.1016/j.pmatsci.2023.101071

Varun Fotedar. (2022). Why the permeability rate of a polymer material is dependent upon a variety of factors - Packaging South Asia. ⟨https://packagingsouthasia.com/events/tokyo-pack/why-the-permeability-rate-of-a-polymer-material-is-dependent-upon-a-variety-of-factors/⟩.

Walker, T. W., Frelka, N., Shen, Z., Chew, A. K., Banick, J., Grey, S., Kim, M. S., Dumesic, J. A., Van Lehn, R. C., & Huber, G. W. (2020). Recycling of multilayer plastic packaging materials by solvent-targeted recovery and precipitation. *Science Advances, 6*. ⟨https://www.science.org⟩.

Williams, J. L., & Peterlin, A. (1971). Transport properties of methylene chloride in drawn polyethylene as a function of the draw ratio. *Journal of Polymer Science Part A-2: Polymer Physics, 9*(8), 1483–1494. https://doi.org/10.1002/pol.1971.160090808